

# A theory of quantum gravity based on quantum computation

Seth Lloyd

Department of Mechanical Engineering  
MIT 3-160, Cambridge MA 02139 USA  
The Santa Fe Institute  
1399 Hyde Park Road, Santa Fe, NM 87501 USA

slloyd@mit.edu

## Abstract

This paper proposes a method of unifying quantum mechanics and gravity based on quantum computation. In this theory, fundamental processes are described in terms of pairwise interactions between quantum degrees of freedom. The geometry of space-time is a construct, derived from the underlying quantum information processing. The computation gives rise to a superposition of four-dimensional spacetimes, each of which obeys the Einstein-Regge equations. The theory makes explicit predictions for the back-reaction of the metric to computational ‘matter,’ black-hole evaporation, holography, and quantum cosmology.

Quantum computation can be thought of as a universal theory for discrete quantum mechanics. Quantum computers are discrete systems that evolve by local interactions [1], and every discrete quantum system that evolves by local interactions, including lattice gauge theories, can be simulated efficiently on a quantum computer [2-6] The quantization of gravity remains one of the primary challenges to physics [7-31]. If, at bottom,

quantum gravity is a discrete, local quantum theory, then quantum gravity, too, should be describable as a quantum computation.

Unlike conventional approaches to quantum gravity such as string theory [14], canonical quantization [7], loop quantum gravity [15-20], and Euclidean quantum gravity [10] the theory proposed here does not set out to quantize gravity directly. Gravity is a theory based on geometry and distance: the normal approach to gravity is to quantize the metric of spacetime. In the theory investigated here, the concept of distance is not a fundamental one. Instead, distances are quantities that are derived from the underlying dynamics of quantum systems. For example, a lattice gauge theory can be written as a sum of local Hamiltonians that give interactions between the fields at different points on the lattice. In our theory, rather than regarding the distances between points on the lattice as independent variables, we *derive* those distances from the quantum behavior of the underlying fields. As will be shown below, those derived distances automatically conform to the laws of general relativity: that is, a lattice theory of the standard model can give rise directly to a theory of quantum gravity, without ever explicitly quantizing the gravitational field. Quantum fluctuations in the interactions between fields translate directly into quantum fluctuations in those distances, and consequently in the metric of spacetime. Because distances are derived from dynamics, without reference to an underlying spacetime manifold, the resulting theory is intrinsically covariant and background independent: the observable content of the theory resides in the underlying computation, and is independent of any background or choice of coordinates.

Because of their ability to reproduce the dynamics of discrete quantum systems, including local Hamiltonian systems such as lattice gauge theories, quantum computers will be used here as the fundamental system from which to derive quantum gravity. Phrased in terms of quantum computation, what is quantized is not the metric of spacetime; rather,

what is quantized here is information. All observable aspects of the universe, including the metric structure of spacetime and the behavior of quantum fields, are derived from and arise out of an underlying quantum computation. The form that quantum fluctuations in geometry take can be calculated directly from the quantum computation. To paraphrase Wheeler, ‘it from qubit’ [12-13]. The approach of deriving geometry from the behavior of quantum mechanical matter is reminiscent the work of Sakharov [21]; however, as will be seen, the method presented here for deriving gravity from the underlying quantum dynamics differs from Sakharov’s, and resolves issues such as the back reaction and the coupling of the metric to quantum fluctuations that Sakharov’s theory failed to resolve. Apart from Sakharov, the closest existing approach to the one taken here is that of causal sets [22-26]. (See also [27-28]; for work relating quantum computation to loop quantum gravity see [13,29-30]).

This paper is organized as follows: Section (1) reviews the theory of quantum computation, and shows how a quantum computation can be written as a superposition of computational ‘histories,’ each one of which possesses a definite causal structure and a definite local action. Quantum fluctuations in causal structure and in the local action and energy are determined by the local dynamics of the computation. Section (2) shows that each of these histories, in turn, gives rise to a classical discretized spacetime geometry, whose metric is *deduced* from the causal structure and local action. The superposition of the histories in the quantum computation gives rise to a quantum superposition of spacetimes, whose fluctuations in causal structure and curvature are determined by the same local computational dynamics. Section (3) applies the results of sections (1-2) to analyze the quantum behavior of singularities, black hole evaporation, the quantum back reaction, the holographic principle, and quantum cosmology. These results can be summarized as follows:

- (a) Singularities obey a form of the cosmic censorship hypothesis.
- (b) Black hole evaporation is either unitary or approximately unitary: all or most information escapes from black holes as they evaporate.
- (c) Because distances are determined from underlying quantum dynamics, fluctuations in distance track quantum fluctuations in the computational ‘matter’: a quantum fluctuation in the device that determines distance is indistinguishable from a quantum fluctuation in the distance itself.
- (d) The theory proposed here is consistent with holography and supplies a complementary principle, the quantum geometric limit, which limits the number of elementary events, or ‘ops,’ that can occur within a four-volume of spacetime.
- (e) Finally, simple quantum cosmologies can give rise to primordial, Planck-scale inflation, followed by epochs of radiation dominance and matter dominance; parts of the universe can then begin to re-inflate at a reduced rate determined by the Hubble parameter at that later epoch. The mechanisms for primordial inflation and late-epoch inflation are essentially the same: only the dynamically determined fundamental length scale changes.

## 1 Quantum computation

Quantum computers are devices that process information in a way that preserves quantum coherence. The quantum information that quantum computers process is registered on quantum degrees of freedom, typically a ‘qubit’ with two distinct states such as electron spin or photon polarization.

### 1.1 The computational graph

Each quantum computation corresponds to a directed, acyclic graph  $G$ , the ‘wiring diagram’ for the computation (figure 1). The initial vertices of the graph correspond to

input states. The directed edges of the graph correspond to quantum wires that move quantum information from place to place. The internal vertices of the computational graph represent quantum logic gates that describe interactions between qubits. The final vertices of the graph correspond to output states. Infinite computations correspond to graphs that need not have final states.

The quantum computation gives rise to an amplitude  $\mathcal{A} = \langle 00 \dots 0 | U | 00 \dots 0 \rangle$ , where  $|00 \dots 0\rangle$  is the initial state of the qubits,  $U = U_n \dots U_1$  is the unitary operator given by the product of the unitary operations  $U_\ell$  corresponding to the individual quantum logic gates that act on the qubits one or two at a time, and  $\langle 00 \dots 0 |$  is the final state (figure 1). Infinite computations do not possess an overall amplitude, but still assign conditional amplitudes to transitions between states within the computation.

*Example: quantum simulation*

As noted above, quantum computation can reproduce the behavior of any discrete quantum mechanical system [2-6]. Let's review how a quantum computer can reproduce the dynamics of a quantum system, such as a lattice gauge theory, whose dynamics consists of Hamiltonian interactions between discrete degrees of freedom. Consider a Hamiltonian of the form  $H = \sum_\ell H_\ell$ , where each Hamiltonian  $H_\ell$  acts on only a few degrees of freedom, e.g., fields at neighboring lattice sites. Using the Trotter formula, the time evolution of this Hamiltonian can be written

$$e^{-iHt} = e^{-iHt/n} \dots e^{-iHt/n} = \Pi_\ell e^{-iH_\ell t/n} \dots \Pi_\ell e^{-iH_\ell t/n} + O(\|Ht\|^2/n). \quad (1)$$

so that the overall time evolution can be approximated arbitrarily accurately using a sequence of local transformations simply by slicing time finely enough [3]. Now each  $e^{-iH_\ell t/n}$  can be enacted using only a small number of quantum logic gates:  $e^{-iH_\ell t/n} \approx U_m \dots U_1$ . Here the number of logic gates  $m$  required to approximate  $e^{-iH_\ell t/n}$  to accuracy

$\epsilon$  goes as  $\epsilon^{-d^2}$ , where  $d$  is the dimension of the local Hilbert space acted on by  $H_\ell$ . (For example, for pairwise interactions between two-level systems,  $d = 4$ .) The logic gates  $U_k$  used to enact the infinitesimal time evolutions  $e^{-iH_\ell t/n}$  can themselves involve only infinitesimal rotations in Hilbert space.

Accordingly, any local Hamiltonian dynamics, including, e.g., lattice gauge theory, can be reproduced to any desired degree of accuracy using a sequence of infinitesimal quantum logic operations [3]. Indeed, a lattice gauge theory can be thought of as a special case of a quantum computation, in which the quantum degrees of freedom are the quantum fields at different lattice points, and the quantum logic gates are infinitesimal Hamiltonian interactions coupling fields at the same point or at neighboring points. Fermionic systems can be reproduced either by quantum computations that use fermionic degrees of freedom [5], or by local interactions that reproduce fermionic statistics [4,6,31]. As a result, the techniques given here to derive quantum gravity from the sequence of quantum logic operations in a quantum computation will serve equally well to derive a theory of quantum gravity from the sequence of infinitesimal Hamiltonian interactions in a lattice gauge theory such as the standard model. In the former case, the concept of distance is derived from the interactions between qubits; in the latter, it is derived from the interactions between quantum fields.

## 1.2 Computational histories

In the computational universe, the structure of spacetime is derived from the behavior of quantum bits as they move through the computation. At each vertex of the computational graph, depending on the state of the incoming quantum bits, those qubits can either be transformed (scattering), or not (no scattering). When qubits scatter, that constitutes an event. If the bits are not transformed (no scattering), then there is no way to tell that

they have interacted: no scattering, no event. Each computation is a superposition of different computational histories, one for each pattern of scattering events (figures 2 and 3).

A scattering/no-scattering superposition in the computation corresponds to a fluctuation in the path that information takes through the computation. Because such an event/no-event superposition is a superposition of different causal structures, it will be seen below to correspond to a fluctuation in spacetime geometry. To make this ‘scattering – no scattering’ picture explicit, consider quantum logic gates of the form  $U = e^{-i\theta P}$ , where  $P^2 = P$  is a projection operator. In this case,  $P(1) \equiv P$  projects onto the eigenspace of  $U$  with energy 1, and  $P(0) \equiv 1 - P$  projects onto the eigenspace with energy 0.  $U$  can be written as  $U = P(0) + e^{-i\theta}P(1)$ : states in the 0 eigenspace of  $P$  do not interact (no scattering), while states in the 1 eigenspace interact and acquire a phase  $e^{-i\theta}$  (scattering). For example, if  $P$  is the projector onto the two-qubit triplet subspace, then  $U = e^{-i\theta P}$  continuously ‘swaps’ the input qubits; such transformations are universal on a subspace of Hilbert space [32-33].

The generalization to quantum logic gates with more than one non-zero eigenvalue is straightforward (see Methods A1.2): in this case, each non-zero eigenvalue corresponds to a scattering event, but different eigenvalues gives rise to a different phase associated with the vertex. If there are no non-zero eigenvalues, then all computational histories have the same causal structure, but differ in the action associated with each vertex.

The vertices of a computational history correspond to scattering events. A computation with  $n$  logic gates gives rise to  $2^n$  computational histories  $C_b$ , where  $b = b_1 \dots b_n$  is an  $n$ -bit string containing a 1 for each scattering event and a 0 for each non-scattering non-event. The overall unitary transformation for the computation,  $U = U_n \dots U_1$ , can

be decomposed in to a sum over the  $2^n$  computational histories  $C_b$ :

$$\begin{aligned}
 U_n \dots U_1 &= (P_n(0) + e^{-i\theta_n} P_n(1)) \dots (P_1(0) + e^{-i\theta_1} P_1(1)) \\
 &= \sum_{b_n \dots b_1 = 00 \dots 0}^{11 \dots 1} e^{-i \sum_{\ell} b_{\ell} \theta_{\ell}} P_n(b_n) \dots P_1(b_1). \quad (1.1) \quad (2)
 \end{aligned}$$

Each computational history  $C_b$  has a definite phase  $e^{-i\theta_{\ell}}$  associated with each scattering event  $b_{\ell} = 1$  (figures 2 and 3). Here,  $\theta_{\ell}$  is the phase acquired by the nonzero-energy eigenstate of the  $\ell$ 'th quantum logic gate:  $\theta_{\ell}$  is an angle rotated in Hilbert space. Define the *action* of a computational history  $C$  to be  $I = \hbar \sum_{\ell \in v(C)} \theta_{\ell}$ , where  $v(C)$  are the vertices of  $C$ . If we think of each quantum logic gate as supplying a local interaction at a scattering event, then  $\hbar\theta_{\ell}$  is equal to the energy of interaction times the time of interaction. Because in quantum mechanics only *relative* phases are observable, we take the lowest energy eigenstate to have eigenvalue 0, and the phases  $\theta_{\ell}$  to be positive.

A quantum computation is a superposition of computational histories. As will now be shown, each computational history corresponds to a discrete classical spacetime with a metric that obeys the discrete form of Einstein's equations. The superposition of computational histories then gives rise to a superposition of classical spacetimes, like the superposition of paths in a path integral.

## 2 General relativity and Regge calculus

Einstein derived the theory of general relativity from the principle of general covariance [34]: the laws of gravitation should take the same form no matter how one chooses to assign coordinates to events. To relate quantum computation to general relativity, embed the computational graph in a spacetime manifold by mapping  $C$  into  $R^4$  via an embedding mapping  $\mathcal{E}$ . Vertices of the embedded graph correspond to events, and wires correspond to the paths information takes in the spacetime. The embedding mapping should respect

the causal structure of  $C$ : because it is a directed, acyclic graph,  $C$  contains discrete analogs of Cauchy surfaces, sets of points which non-extensible causal paths intersect exactly once. The embedding should map each discrete Cauchy set of  $C$  into a Cauchy surface of the spacetime; and a foliation of  $C$  in terms of discrete Cauchy sets should be mapped into a foliation of the spacetime in terms of Cauchy surfaces.

The geometry of the spacetime is derived from the embedded computation. The information that moves through the computation effectively ‘measures’ distances in spacetime in the same way that the signals passed between members of a set of GPS satellites measure spacetime. The observational content of a quantum computation consists of its causal structure together with the local action of the computation. Each computational history gives rise to a particular causal structure, embodied in the history’s directed graph, and a particular phase or action associated with each vertex of that directed graph. All other quantities, such as edge lengths, curvature, and the stress-energy tensor, are to be deduced from this causal structure and action.

Since the way that information is processed in a quantum computation is independent of the way in which that computation is embedded in spacetime, any dynamical laws that can be derived from the computation are automatically generally covariant and background independent: the observational content of the theory (causal structure and action) is invariant under general coordinate transformations. Since general covariance (together with restrictions on the degree of the action) implies Einstein’s equations, the geometry induced by the computational universe obeys Einstein’s equations (in their discrete, Regge calculus form [35-37]). We now verify this fact explicitly.

## 2.1 Regge Calculus

Because the computational graph is at bottom a lattice picture of spacetime, the computational universe is based on the Regge calculus version of general relativity [35-37]. In Regge calculus, spacetime geometry is defined by a simplicial lattice whose edge lengths determine the metric and curvature. This simplicial lattice is a discrete, ‘geodesic dome’ analog of the manifold. Each computational history  $C_b$  gives rise to a Regge calculus by the following steps. The computation as a whole corresponds to a superposition of Regge calculi, one for each computational history.

The lattice determined by a given computational history  $C$  is not itself simplicial. Extend it to a simplicial Delaunay lattice  $D_C$  by adding edges and vertices [38]. All edges of the computational history are edges of the simplicial lattice (they may be divided into several segments by additional vertices). The four edges at each vertex of the computational graph, two incoming and two outgoing, define a four-simplex associated with each vertex: the pairwise nature of interactions between quantum degrees of freedom gives rise naturally to a four-dimensional discrete geometry [figure 4].

There are a variety of methods for extending a lattice to form a simplicial lattice [38]; two are described in the Methods. *No matter how one constructs such an extension, the resulting discrete spacetime still possesses the same observable content.* The causal structure and action of the discretized spacetime depend only on the computational history  $C$ , and not on the choice of simplicial lattice used. That is, the microscopic details of  $D_C$  do not affect the observable structure of spacetime. Just as two surveyors can triangulate the same landscape in different ways, and yet obtain the same geometry for the region, so two different simplicial triangulations of the computational history possess the same causal structure and action. Consequently, as will be seen below, different triangulations also give rise to the same curvature associated with a vertex.

The simplicial lattice  $D_C$  gives the edges of a four-dimensional geodesic dome geometry, and its dual lattice  $V_C$  defines the volumes  $\Delta V_\ell$  associated with the vertices. The simplicial lattice corresponds to a four-dimensional Lorentzian spacetime [35-37]. In the usual construction of Regge calculus, the variables that define the geometry are the lengths of the edges of the simplicial lattice. In the computational theory considered here, these lengths are defined by the dynamics of the computation. Along wires, no phase is accumulated and the action is zero. Accordingly, identify these wires with null lines  $E_a$ , for  $a = 1$  to 4.

Embedding a vertex and its neighbors in  $R^4$  and using these four null lines  $E_a$  as a null basis implies that the on-diagonal part of the metric is zero:  $g_{aa} = g(E_a, E_a) = 0$ . (If the  $E_a$  are not linearly independent, almost any small change in the embedding will make them so.) The off-diagonal part of the metric is to be determined by a requirement of self-consistency. Once one picks the off-diagonal parts of the metric at each vertex, the length of each edge is fixed by averaging the lengths given by the metrics on the two vertices associated with the edge. That is, the length of the edge  $l$  connecting vertices  $j$  and  $k$  is equal to  $g_{ab}(j)l^a l^b / 2 + g_{ab}(k)l^a l^b / 2$ . This definition of edge length is covariant. To enforce the requirement of self-consistency, assume that the full metric has been chosen at each point, so that edge lengths and the full geodesic dome geometry are fixed. As in the reconstruction of the discrete metric from GPS data, the causal structure and local action will then determine a self-consistent choice of the off-diagonal terms of the metric.

Once the off-diagonal terms have been chosen, Miller's elegant construction of the connection and curvature tensor for Regge calculus on Delaunay and Voronoi lattices can be applied [36]. In four dimensional Regge calculus, curvature lies on triangular hinges. Once the edge lengths have been defined, each hinge has a well-defined curvature, volume, and action associated with it. The gravitational action corresponding to a hinge is just

$(1/8\pi G)A\epsilon$ , where  $A$  is the area of the hinge and  $\epsilon$  is the deficit angle of the hinge. The action corresponding to a hinge is invariant under coordinate transformations.

## 2.2 The Einstein-Regge equations

The Einstein-Regge equations are obtained by demanding that the combined action of gravity and matter are stationary under variations of the metric [39]. The usual way of deriving the Einstein-Regge equations is to demand that the action be stationary under variations in the individual edge lengths:  $\delta I/\delta l(jk) = 0$ . The edge lengths determine the metric, and *vice versa*, so stationarity under variations in the edge lengths is equivalent to stationarity under variation in the metric,  $\delta I/\delta g_{ab}(j) = 0$ .

The action of the gravitational degrees of freedom in Regge calculus is a scalar quantity given by the sum of the actions over the individual hinges:  $I_G = (1/8\pi G)\sum_h A_h\epsilon_h$ , where  $G$  is the gravitational constant. For finite computations this action should be supplemented with a term,  $(1/8\pi G)\sum_k B_k\beta_k$ , corresponding to the extrinsic curvature of the three dimensional boundary of the computation [40-41]. Here,  $B_k$  is the area of the  $k$ 'th triangle joining two tetrahedra at the boundary of the lattice, and  $\beta_k$  is the angle between the normals to those two tetrahedra.  $A_h$  and  $\epsilon_h$  are functions of the metric at that point and at neighboring points. Define the action of the computational matter to be the scalar quantity  $I_M = -\hbar\sum_{\ell\in v(C)}\theta_\ell$ , proportional to the overall action  $I$  of the computational history. The Einstein-Regge equations at a point  $\ell$  are then given by

$$\delta I_G/\delta g_{ab}(\ell) + \delta I_M/\delta g_{ab}(\ell) = 0. \quad (3)$$

In the Lagrangian approach to general relativity  $\delta I_G/\delta g_{ab}(\ell)$  is equal to  $(-1/16\pi G)\Delta V_\ell$  times the discretized Einstein tensor,  $G^{ab} = R^{ab} - (1/2)g^{ab}R$ ; similarly,  $\delta I_M/\delta g_{ab}(\ell)$  is equal to  $(1/2)T^{ab}\Delta V_\ell$  where  $T^{ab}$  is the energy-momentum tensor ([39] section 3.3). Here,  $\Delta V_\ell$  is the Voronoi volume at point  $\ell$ .

To obtain an explicit form for the Einstein-Regge equations, write the action for the computational matter  $I_M = -\hbar \sum_{\ell \in v(C)} \theta_\ell$  as  $\sum_\ell \mathcal{L}_\ell \Delta V_\ell$  where  $\mathcal{L}_\ell$  is the local Lagrangian at point  $\ell$ . Following Einstein and taking the Lagrangian to be a function only of the computational ‘matter’ together with the metric to first order, we have

$$\mathcal{L}_\ell = -g_{ab} \hat{T}^{ab} / 2 - \mathcal{U}_\ell, \quad (4)$$

where  $\hat{T}^{ab} = \text{diag}(\gamma_1, \gamma_2, \gamma_3, \gamma_4)$  is diagonal in the null basis, so that  $g_{ab} \hat{T}^{ab} = 0$ . Here,  $\mathcal{U}_\ell$  is the energy density of the interaction between the qubits at the  $\ell$ 'th quantum logic gate; it gives the potential energy term in the energy momentum tensor. As will be seen below,  $\hat{T}^{ab}$  represents the kinetic energy part of the energy momentum tensor, and  $\gamma_a$  is the energy density of the ‘particle’ moving along the vector  $E_a$ .  $\hat{T}^{ab}$  is a traceless tensor that does not contribute to the action, but does contribute to the energy-momentum tensor. For the moment, the  $\gamma_a$  are free parameters: since the choice of the  $\gamma_a$  does not affect the action, they can be chosen in a suitable way, e.g., to make the Einstein-Regge equations hold.

The computational ‘matter’ looks like a collection of massless particles traveling along null geodesics and interacting with each other via two-particle interactions at the quantum logic gates.  $\hat{T}^{ab}$  is the kinetic energy term for these massless particles, and  $\mathcal{U}$  is the potential energy term. This relation of this ‘quantum computronium’ to conventional quantum fields will be discussed below. Note that ordinary matter seems to have  $T^a_a \leq 0$ , corresponding to non-negative energies and phases  $\theta_\ell$  for the quantum logic gates.

The Einstein-Regge equations (2.1) now take the explicit form (Methods A2.2):

$$-\sum_{h \in N(\ell)} \epsilon_h \frac{\delta A_h}{\delta g_{ab}(\ell)} = 4\pi G T^{ab} \Delta V_\ell \quad (5)$$

where the energy-momentum tensor  $T^{ab} = \hat{T}^{ab}(\ell) - \mathcal{U}_\ell g^{ab}(\ell)$ . Here, the sum over hinges

includes only hinges  $h \in N(\ell)$  that adjoin the vertex  $\ell$ , as the edges of other hinges do not change under the variation of the metric at  $\ell$ .

Equations (2.3) are the form for the Einstein-Regge equations in the computational universe (they can also be written in terms of edge lengths and angles as in [35], Methods A2.2). Just as in the ordinary Einstein equations, the left-hand side of (2.3) contains only geometric terms, while the right-hand side contains terms that depend on the action of the computational matter and on the metric to first order. The terms on the left hand side of equation (2.3) are functions of  $g_{ab}$  at  $\ell$  and at adjacent points. The right hand side of (2.3) depends only on the computational ‘matter.’ In other words, equation (2.3) is a nonlinear partial difference equation that relates the curvature of space to the presence of matter, with the local phase of the computational matter acting as a source for curvature. The computational matter tells spacetime how to curve.

Now we can verify that the gravitational action associated with a vertex is independent of the embedding and simplicial extension. Taking the trace of equation (2.3) yields  $R_\ell \Delta V_\ell = 32\pi G \hbar \theta_\ell$ , where  $R_\ell \Delta V_\ell / 16\pi = I_{G\ell} = 2\hbar \theta_\ell$  is the action of the gravitational field associated with the point  $\ell$ . In other words, like the action of the computational ‘matter,’ the gravitational action is just proportional to the angle rotated at the vertex; it is a scalar quantity that is invariant under embedding and simplicial extension. Up until now, we have been associating the computational action at each vertex with the action of the ‘matter’ fields alone. However, since  $I_{G\ell} = 2\hbar \theta_\ell$ , we can associate the computational action with *both* matter and gravity. Indeed, the total action of matter and gravity associated with the  $\ell$ 'th vertex is just the computational action  $I = I_{M\ell} + I_{G\ell} = -\hbar \theta_\ell + 2\hbar \theta_\ell = \hbar \theta_\ell$ . The dynamics of the quantum computation give rise both to matter and to gravity, coupled together.

As in [35], when the average curvature of the simplicial lattice is small, corresponding

either to length scales significantly larger than the Planck scale, or to small angles rotated at each vertex, the ordinary Einstein equations can be obtained from equations (2.3) by a process of coarse-graining (Methods section A2.2-3). Note that in the example given above of a quantum computer reproducing the dynamics of a system with a local Hamiltonian such as lattice gauge theory, the angles rotated at each vertex are indeed small, so that in this case coarse-graining may be expected to give an accurate reproduction of the underlying discrete dynamics.

### 2.3 Satisfying the Einstein-Regge equations

The Einstein-Regge equations (2.3) govern the self-consistent assignment of lengths in the simplicial geometry. In order to complete the construction of discrete geometry from an underlying computational history, the parameters that so far have remained free must be fixed. These parameters are the off-diagonal part of the metric, and the on-diagonal part of the energy-momentum tensor. Self-consistency dictates that these parameters be chosen in such a way that equations (2.3) are satisfied.

Equations (2.3) express the relationship between matter and geometry for one computational history in the discrete, computational universe. They are a set of ten coupled, nonlinear difference equations which can be solved (e.g., numerically) given appropriate boundary conditions. To fix the free parameters, first choose the six off-diagonal terms in the metric to satisfy the off-diagonal part of equation (2.3). Next, choose the four on-diagonal terms in the energy-momentum tensor,  $\gamma_a$ , so that remainder of the Einstein-Regge equations (2.3) are obeyed. The four on-diagonal terms  $\gamma_a$  correspond to the ‘kinetic energies’ of the four qubits as they move through the computation. Essentially, choosing  $\gamma_a$  in this fashion reduces to insisting that energy and momentum travel along the null geodesics specified by the causal structure, and demanding that  $T^{ab}{}_{;b} = 0$ . The

traceless part of the gravitational terms in the Einstein-Regge equations can be thought of as source terms that determine the kinetic energy of the computational matter: spacetime tells qubits where to go.

At reference vertices and at vertices corresponding to single-qubit logic gates, fewer null lines are determined by the computational history. As shown in Methods, section A2.3, the Einstein-Regge equations can still be used to satisfy the self-consistency conditions at such vertices.

This completes the construction: each computational history gives rise to a discrete geometry that obeys the Einstein-Regge equations.

## 2.4 2.4 Minimum length scale is the Planck scale

Because only relative phases are observable, we have adopted the convention that local phases and curvature are positive:  $\epsilon_h > 0, \theta_\ell > 0$ . Consequently, a minimum length scale arises because the maximum positive deficit angle is  $\epsilon_h = 2\pi$ . In equation (2.3), the curvature terms are on the order of  $\epsilon_h A_h$ , while the minimum phase  $\theta_\ell$  required to flip a qubit is  $\pi$ . As a result, if area of a hinge  $A_h$  adjacent to an event in which a bit flips is less than the Planck area  $\approx \hbar G$ , it is not possible to satisfy (2.3): space would have to curve more than it can curve.

If we relax the assumption of positive phases and curvature, ( $\epsilon_h < 0, \theta_\ell < 0$ ), this argument does not seem to apply, as there is no limit on how negative the deficit angle can be. As noted above, however, ordinary matter seems to have  $T^a_a \leq 0$ , corresponding to non-negative local phases, energies, and curvatures.

### 3 Observational consequences of the computational universe.

The previous section showed how each computational history gives rise to a classical discrete spacetime that obeys the Einstein-Regge equations. As shown in section (1), a quantum computation is a superposition of computational histories, and so gives rise to a superposition of spacetimes. Now investigate the implications of the computational universe picture for several well-known problems in quantum gravity.

#### 3.1 The back reaction

The first problem for which the computational universe provides an explicit solution is the back reaction of the metric to quantum-mechanical matter [7]. Here, since the metric is derived from the underlying dynamics of quantum information, its fluctuations directly track the quantum fluctuations in the computational matter. In particular, fluctuations in the curvature scalar track the fluctuations in the local phase or action accumulated by the computational matter; and quantum fluctuations in the routing of signals through the computation (via scattering or lack of scattering) give rise to fluctuations in the remainder of the metric. For example, such fluctuations can give rise to gravity waves via the usual mechanism in which the Ricci tensor and curvature scalar act as source terms for gravity waves in classical relativity via the Bianchi identities ([39] section 4.1).

The computational universe model is intrinsically a theory of quantum matter *coupled* to gravity, and not a theory of either quantum matter or quantum gravity on its own. But it still supports such ‘purely gravitational’ effects as gravity waves. A computation that contains a binary pulsar will also contain the gravity waves emitted by that pulsar. Quantum fluctuations in the positions and momenta of the two stars that make up the pulsar will give rise to fluctuations in the gravity waves emitted. Those gravity waves

will propagate through the computational vacuum and will induce disturbances in the computational cosmic background radiation; finally, if the computation contains LIGO, it will detect those gravity waves.

The intertwined nature of quantum matter and quantum metric in this theory implies that when the matter decoheres (see section (3.5) below), so does the metric. But the metric does not independently act as a source of decoherence for the underlying quantum mechanical matter (in contrast with [11, 42]). Consequently, the experiment proposed in [42] should reveal no intrinsic decoherence arising from the self-energy of the gravitational interaction.

### **3.2 Singularities and black hole evaporation**

Initial singularities in the computational universe correspond to places in the computation where bits are added to the computation, as in section (1.1) above. As soon as a newly minted bit interacts with another bit, a new volume of spacetime is created; its size is determined by solving equation (2.3). Similarly, final singularities occur when bits leave the computation, corresponding to a projection onto a final bit, also as in (1.1). When the bits go away, so do the volumes of spacetime associated with them. Initial and final singularities are essentially the time reverse of each other; they are quite ‘gentle’ compared with our normal view of such singularities. Although the energy scales associated with such singularities can be high, the process of bits entering and leaving the computation is orderly and quantum-mechanically straightforward.

Singularities obey a version of the cosmic censorship hypothesis. Final singularities occur at points where bits go away: there are no future directed ‘wires’ leading away from them. Similarly, initial singularities occur at points where bits come into existence: there are no past directed wires leading into them.

The behavior of the computation at final singularities gives rise to a mechanism for information to escape from black holes. In a finite computation with projection onto final states  $\langle 00 \dots 0 |$ , black hole evaporation can take place by a variant [43] of the Horowitz-Maldacena mechanism [44]. As shown in [43-47], some, and typically almost all, of the quantum information in a black hole escapes during the process of evaporation. If microscopic black holes can be created experimentally, e.g., in high-energy collisions, the theory predicts that their evaporation should be approximately unitary.

### 3.3 Holography and the geometric quantum limit

In the case that local energies and phases are taken to be positive, the geometric quantum limit [48] bounds the number of elementary events (ops) that can be fit into a four volume of spacetime to  $\# \leq (1/2\pi)(x/\ell_P)(t/t_P)$ , where  $x$  is the spatial extent of the volume and  $t$  is the temporal extent. The geometric quantum limit is consistent with and implies holography [48-51]. A detailed description of the geometric quantum limit and its relation to holography can be found in reference [48].

Note that the geometric quantum limit implies that the separations between bits and quantum logic operations within a volume of space time are typically much greater than the Planck length. In particular, for our universe as a whole, the total number of ops and bits is less than or equal to  $t^2/t_P^2 \approx 10^{122}$ . This yields an average spacing between ops in the universe up to now of  $\sqrt{tt_P} \approx 10^{-13}$  seconds. (As will be seen below, this time scale can be related to the mass scale for fundamental spinors.) Of course, here on Earth, where matter is packed more densely than in the universe as a whole, bits and ops are crammed closer together.

### 3.4 Quantum cosmology

The Einstein-Regge equations (2.3) can be solved under certain simplifying assumptions (e.g., large computations with random wiring diagrams, or uniform, cellular-automaton type architectures) to calculate the spectrum of curvature fluctuations in the early universe [52]. The approximate spatial homogeneity of random and CA-like architectures gives an approximately homogeneous, isotropic universe in which the Einstein-Regge equations take on a Friedmann-Robertson-Walker form. Note that cellular automata may not be isotropic: particular directions may be picked out by the axes of the automaton. However, the example of lattice gases shows that such architectures can still give rise to an isotropic dynamics at a coarse-grained level. In particular, if the underlying dynamics is that of lattice QCD, we expect the coarse-grained dynamics to be isotropic.

For homogeneous, isotropic spacetimes, the coarse-grained metric (averaging over microscopic fluctuations) takes on the form [39]

$$ds^2 = -dt^2 + a^2(t)(d\chi^2 + f^2(\chi)(d\theta^2 + \sin^2\theta d\phi^2)). \quad (6)$$

Here  $f(\chi) = \sin \chi$  for three spaces of constant positive curvature,  $f(\chi) = \chi$  for three spaces of zero curvature, and  $f(\chi) = \sinh \chi$  for three spaces of constant negative curvature. The homogeneity of the spacetime requires the energy momentum tensor of the matter to take on the form of a perfect fluid, with energy density  $\rho$  and pressure  $p$ . The Friedmann-Robertson-Walker (FRW) equations then take on the form

$$\dot{\rho} = -3(\rho + p)\dot{a}/a \quad (7)$$

$$4\pi G(\rho + 3p)/3 = -\ddot{a}/a \quad (8)$$

$$8\pi G\rho/3 = \dot{a}^2/a^2 - k/a^2, \quad (9)$$

where  $k = -1, 0, +1$  for three spaces of positive curvature, zero curvature, and negative

curvature, respectively. The third of these equations is just the integral of the first, so there are really only two independent FRW equations.

Recall that our prescription is first to assign the free parameters of the metric so that the off-diagonal, potential energy ( $U$ ) parts of the Einstein-Regge equations hold, and then to assign the kinetic energy terms so that the on-diagonal parts of the equations hold. Under the assumptions of homogeneity and isotropy, the potential energy part of the energy-momentum tensor takes on the form  $diag(U, -U, -U, -U)$ , while the (traceless) kinetic energy part takes on the form  $diag(K, K/3, K/3, K/3)$ , so that  $\rho = K + U$ , and  $p = K/3 - U$ . Defining the Hubble parameter  $H = \dot{a}/a$ , we can rewrite the FRW equations (3.2) as

$$16\pi GU/3 = \dot{H} + 2H^2 \quad (3.3a) \quad (10)$$

$$8\pi G(K + U)/3 = H^2 - k/a^2. \quad (3.3b) \quad (11)$$

Recall that the potential associated with a four volume of spacetime  $\Delta V$  is  $U = \hbar\theta/\Delta V$ , where  $\theta$  is the net phase acquired within  $\Delta V$ . Fixing  $a$  fixes the scale of the volume  $\Delta V$ . Accordingly, for a given underlying computational geometry, equation (3.3a) can be regarded as a differential equation in  $a$ . Once this equation is solved, the kinetic energy  $K$  can be assigned according to equation (3.3b).

Let's look at some different possible behaviors of the FRW equations in the computational universe. The FRW equations can conveniently be rewritten as

$$-16\pi GK/3 = \dot{H} \quad (3.4a) \quad (12)$$

$$8\pi G(K + U)/3 = H^2 - k/a^2. \quad (3.4b) \quad (13)$$

First, consider the case of a flat universe,  $k = 0$ . The case of positive intrinsic curvature,  $k = -1$ , will be investigated below. (Note that the positivity of energy requires  $H > 1$  for

a universe with negative curvature  $k = 1$ .) We can distinguish between several different regimes.

- First, take the case  $K = 0$ . Then  $\dot{H} = 0$ ,  $H$  equals a constant, as does  $U$ , and the universe undergoes inflation at a constant rate:  $a(t) = a(0)e^{\alpha t}$ .
- If  $U \gg K$ , then the universe also expands exponentially; but as long as  $K > 0$ , equation (3.4a) shows that the rate of expansion to decreases over time. Since  $\ddot{a}/a = 8\pi G(U - K)/3$ , when  $K > U$ , then  $\ddot{a} < 0$ , and the universe ceases to inflate.
- The situation  $K \gg U$  corresponds to a radiation dominated universe, and equations (3.4) have the solution  $a(t) \propto t^{1/2}$ .
- The situation  $K \approx 3U$  corresponds to a matter dominated universe ( $p = K/3 - U \approx 0$ ), and equations (3.4) have the solution  $a(t) \propto t^{2/3}$ .

All of these scenarios are possible depending on the underlying computation; and each of these scenarios can hold at different stages in the same computation. For example, consider a homogeneous, isotropic computation commencing at  $t = 0$ . In order to solve equation (3.3a), initial conditions on  $a$  and  $K$  must be set. A natural choice is  $a = 1$  (in Planck units) and  $K = 0$ . These initial conditions correspond to the first scenario above, inflation at the Planck rate. Just as in conventional inflation, microscopic fluctuations in local phases give rise to Gaussian curvature fluctuations at the coarse-grained scale, which in turn should be inflated as in the conventional picture of the growth of quantum-seeded curvature fluctuations.

Now equation (3.4a) shows that this inflation is unstable: in any region where the kinetic energy is not strictly zero, the rate of inflation decreases. The greater the kinetic energy in some region, the more rapid the slowdown. In regions where  $K$  grows to be greater  $U$ ,  $\ddot{a}$  becomes less than 0 and inflation stops. Where does this kinetic energy come from? At microscopic scales, homogeneity is broken by quantum fluctuations in the phases

$\theta$  acquired in individual gates. Accordingly, even if the kinetic energy terms in the energy-momentum tensor are initially zero everywhere, the full, microscopic solution of equations (2.3) will give rise to kinetic energy locally. Inflation will then slow, and energetic matter will be created. In other words, just as in the standard picture of inflation, Planck-scale inflation is unstable to the creation of ordinary matter, which nucleates a phase transition and gives rise locally to a radiation-dominated universe.

Uncovering the details of this phase transition will require the detailed solution of equation (2.3), and is beyond the scope of the current paper. Within the confines of the assumption of homogeneity and isotropy, the FRW equation nonetheless can provide useful qualitative information about the behavior of computational cosmologies. For example, consider a radiation dominated universe such as the one created after inflation in the previous paragraph. The kinetic energy density in such a universe drops over time as  $K \propto 1/a^4 \propto t^{-2}$ , while the potential energy density  $U$  is proportional to the density of logic gates and goes as  $U \propto 1/a^3 \propto t^{-3/2}$ . Eventually  $K$  lowers to the level  $K = 3U$  and the universe becomes matter dominated. Not surprisingly, since a homogeneous computation such as a quantum cellular automaton can give rise to conventional matter and energy, and since a homogeneous, isotropic computational universe obeys the FRW equations, the usual picture of a radiation-dominated universe giving way to a matter-dominated one holds in the computational universe.

By the time radiation domination has given way to matter domination, the universe is no longer homogeneous: significant clumping has taken place. Therefore, in addition to matter-dominated regions, we expect some regions to have  $U < K < 3U$ . These regions exhibit negative pressure  $p = K/3 - U$ , but do not have  $\ddot{a} > 0$ : the negative pressure is not great enough for them to inflate. Depending on the scale of the inhomogeneities, other regions may have  $K < U$ . As (3.2b) shows, these regions will begin to undergo

inflation again, though at a rate much smaller than the Planck scale.

We see that at this late date, the computational universe can contain regions dominated by three different types of energy: (1) ordinary matter and radiation,  $K \geq 3U$ , (2) matter (cold dark matter?) with negative pressure that does not inflate,  $U \leq K < 3U$ , and (3) ‘dark energy’ that undergoes inflation,  $K < U$ . The relative preponderance of these regions depends on how inhomogeneities develop in the full Einstein-Regge equations (2.3), and lies beyond the scope of this paper. From continuity, we expect that matter of type 2 should lie in regions such as the halos of galaxies intermediate between ordinary matter (type 1) and dark energy (type 3) (this is the reason for the speculative identification of matter of type 2 with cold dark matter). In accordance with equation (3.3b), in a flat universe, the total density of all three types of matter is equal to the critical density  $3H^2/8\pi G$ . That is, in a universe dominated by dark energy after the radiation and matter-dominated epochs, the rate of inflation is determined by the Hubble parameter at that epoch. In this picture, we see that primordial inflation and late-epoch re-inflation are caused by the same mechanism, a locally potential dominated universe. Because length scales are dynamically determined, however, the rate of late-epoch inflation can be many orders of magnitude (e.g.  $10^{60}$  times) smaller than the rate of primordial inflation.

### 3.5 Universes with positive intrinsic curvature

Let us look at a specific example of a FRW cosmology in the computational universe. In our model, curvature is non-negative. If the underlying computation has approximately uniform distribution of quantum gates, then we are led to consider models with constant positive curvature, i.e., de Sitter space [39]. De Sitter space has topology  $R^1 \times S^3$  and can be visualized as a hyperboloid  $-v^2 + w^2 + x^2 + y^2 + z^2 = \alpha^2$  embedded in flat  $R^5$ , with metric

$ds^2 = -dv^2 + dw^2 + dx^2 + dy^2 + dz^2$ . We can arrange gates uniformly on this hyperboloid with wires following null lines of the metric. The constant curvature of de Sitter space is  $R = 12/\alpha^2$ . The energy momentum tensor is purely potential:  $K = 0$ ,  $U = R/32\pi G$ . Consider gates that correspond to swaps or to bit flips, so that  $U\Delta^4V = \pi\hbar/2$ . Since  $U = 3/8\pi G\alpha^2$ , the spacing between gates is  $(\Delta^4V)^{1/4} = (4\pi/3)^{1/4}\sqrt{t_P\alpha}$ .

The number of bits on successive three-spheres in the  $v$  direction grows as  $(\alpha^2 + v^2)^{3/2}$ , so this computation involves continual bit creation for positive  $v$ , and continual bit destruction for negative  $v$ . The positive  $v$  and negative  $v$  parts of the computation can be time reversals of each other. Note that the discrete nature of the underlying computation means that it is not necessary for the positive  $v$  part of the computation on the hyperboloid to be causally connected with the negative  $v$  part: there need not be any ‘wires’ passing through the waist at  $v = 0$ . In this case, the  $v \geq 0$  part of the computation can be taken as a model for our universe starting from a big bang.

Setting  $\alpha \sinh(t/\alpha) = v$  and using angular coordinates  $\chi, \theta, \phi$  for the three sphere gives the metric in FRW form for closed spacelike three spaces ( $k = -1$ ) [39]:

$$ds^2 = -dt^2 + \alpha^2 \cosh^2(t/\alpha)(d\chi^2 + \sin^2\chi(d\theta^2 + \sin^2\theta d\phi^2)). \quad (14)$$

De Sitter space expands exponentially at a rate determined by  $\alpha$ .

The qualitative discussion of flat FRW spaces given also holds for this de Sitter space computation. In particular, suppose that  $\alpha$  is taken to be equal to 1, yielding Planck scale inflation. If the distribution of phases rotated in the gates were exactly uniform, then this inflation would continue for ever, and the de Sitter picture would be essentially exact. However, just as before, Planck scale inflation is unstable to the creation of kinetic energy, which slows the rate of expansion. In other words,  $\alpha$  cannot be a constant, but changes in time, approaching  $1/H$  at late times, where  $H$  is the phenomenological Hubble parameter.

Just as in the  $k = 0$  FRW picture, the de Sitter model leads to a rate of inflation that can vary dramatically with time, starting at the Planck scale, going away during the radiation- and matter-dominated phases, and re-emerging at the current epoch.

This discussion of cosmology in the computational universe is necessarily qualitative and preliminary: a full discussion will have to await the detailed solution of equations (2.3) in candidate computational cosmologies, e.g., universes in which the local computation corresponds to the standard model. We present this preliminary picture based on the coarse-grained FRW equations simply to show that the computational theory is apparently consistent with observation for underlying homogeneous computations. Though preliminary, this discussion is nonetheless revealing: it suggests both the existence of exotic, negative pressure matter that might be identified with cold dark matter, together with a natural mechanism for the production of dark energy. In addition, the current re-inflation of the universe by dark energy can take place by the same mechanism as primordial inflation, taking into account the renormalization of the fundamental length scale given by the quantum geometric limit of the previous section.

### **3.6 Matter in the computational universe**

Because quantum computations can support any local Hamiltonian dynamics, there are many types of matter that can be supported in the quantum computational model of quantum gravity. For example, the quantum computation could reproduce the standard model as a lattice gauge theory, which would in turn give rise to quantum gravity by ‘constructing’ the distances between lattice points as described in section (2) above.

Any local quantum theory involving pairwise interactions allows the construction of a theory of quantum gravity. This suggests that we should search for quantum computations whose local symmetries can reproduce the standard model. In fact, the ‘swap’ picture

of quantum computation of section 1.2 above possesses a local  $SU(3) \times SU(2) \times U(1)$  symmetry:  $SU(3) \times U(1)$  commutes with the action of the gates, and  $SU(2)$  commutes with the action of the wires. This symmetry can be promoted to a gauge symmetry by looking at a version of quantum computation that has  $SU(3) \times U(1)$  transformations at the two-qubit gates, and  $SU(2)$  transformations on the wires. The swap picture of quantum computation and the  $SU(3) \times SU(2) \times U(1)$  version are simple and standard pictures of quantum computation. Whether or not they can give rise to the standard model in a simple and straightforward way remains to be seen.

Because the fundamental length scales depend on the cosmological epoch in the computational universe, the masses of some of the elementary particles in the theory are related to cosmological parameters such as the Hubble parameter. In the quantum cellular automaton models of the Dirac equation of Feynman *et. al.* [62-65], the mass of the fundamental Dirac particle is related to the amount of time it takes to accumulate phases in the underlying quantum computation. In particular, in the previous section it was shown both for flat and for closed spatial computational cosmologies, the amount of time it takes to accumulate a phase of  $\pi/2$  is  $\delta t = (4\pi/3)^{1/4} \sqrt{t_P/H}$ . This leads to a mass for the fundamental Dirac particle of  $mc^2 = \pi\hbar/2\delta t \approx 10^{-2}$  eV for the current observed values of  $H$ . This value is consistent with observed constraints on the neutrino mass. Again, whether or not this is a coincidence will have to await a detailed calculation with exact microscopic models.

### 3.7 Decoherent histories and the emergence of classical space-time

In the computational universe, the emergence of the classical world can be described using the decoherent histories approach [53-61] to quantum cosmology proposed by Gell-Mann

and Hartle [55]. In this approach, one assigns amplitudes to histories of hydrodynamic variables such as local energy density, momentum density, etc. A natural application of decoherent histories to the computational universe picture is to take the analog of hydrodynamic variables to be averages  $\bar{T}_{ab}$  of the components of  $T_{ab}$  taken over coarse-grained volumes of space-time. Gell-Mann and Hartle [55] and Halliwell [56] have shown that in many situations, such coarse-grained histories naturally decohere and give rise to classical probabilities for the behavior of the coarse-grained energy-momentum tensor.

Classical spacetime emerges in the computational universe by the combination of the detailed quantum cosmological dynamics discussed above, together with the process of decoherence. As shown, the computational dynamics inflates the computation, spreading out the gates and making the discrete spacetime approximately uniform. In addition, as the computation evolves, different computational histories begin to decohere from each other, giving rise to a semiclassical structure to spacetime.

In the decoherent histories approach [53-61], one constructs a decoherence functional  $D(H, H')$  where  $H$  and  $H'$  are coarse-grained histories of the ‘hydrodynamic’ variables  $\bar{T}_{ab}$ . Hydrodynamic variables arise naturally in the computational universe: indeed, the program for deriving geometry from computation gives rise exactly to a local definition of the energy-momentum tensor  $T_{ab}$ , which yields  $\bar{T}_{ab}$  upon coarse graining.

Each coarse-grained history consists of some ‘bundle’  $C(H)$  of underlying fine-grained computational histories. Each fine-grained computational history within the bundle possesses a definite causal structure, definite local phases, and a uniquely defined  $T_{ab}$  and  $R_{ab}$  that obey the Einstein-Regge equations. The decoherence functional in the path integral formulation [55] can then be defined to be

$$D(H, H') = \sum_{C \in C(H), C' \in C(H')} \mathcal{A}(C) \bar{\mathcal{A}}(C'), \quad (15)$$

where  $\mathcal{A}(C)$  is the amplitude for the computational history  $C$ . Two coarse-grained histories are approximately decoherent if  $D(H, H') \approx 0$  for  $H \neq H'$ . Decoherent histories of hydrodynamics variables behave effectively classically. The visible universe that we see around us presumably corresponds to one such decoherent history.

As an example of the sort of calculation that is possible using the decoherent histories approach, we follow [54-56] to show that coarse-grained histories corresponding to different semi-classical trajectories for spacetime approximately decohere. Semiclassical histories for the energy-momentum tensor correspond to histories which extremize the action. In other words, such semiclassical histories correspond to *stable* computations, in which small changes in the routing of signals through the computation and in the angles rotated at each quantum logic gate do not affect the overall amplitude of the computation to first order. In other words, stable computations are computational analogs of histories that extremize the action.

Such stable computations have a high amplitude by the usual argument: computational histories in the vicinity of a stable history have approximately the same phase, and so positively interfere, leading to a relatively high probability for stable computations. In addition, stability also makes these histories approximately decohere [54-56].

In particular, let  $C(H)$  be the set of fine-grained histories compatible with a particular coarse-grained semiclassical computational history  $H$ . Let  $C(H')$  be the set of fine-grained histories compatible with a different coarse-grained semiclassical history  $H'$  within the same computation. As  $C$  ranges over the fine-grained histories in  $C(H)$ , the phase of  $\mathcal{A}(C)$  oscillates; the phase of  $\mathcal{A}(C')$  oscillates independently. As a result, performing the average over fine-grained histories in equation (A3.9) yields  $D(H, H') \approx 0$  for  $H, H'$  distinct coarse-grained histories corresponding to different causal structures. At the same time, the stability of the histories in  $H$  gives high values of  $D(H, H)$ ,  $D(H', H')$ , thereby satisfying

the condition for approximate decoherence [55-56],  $|D(H, H')|^2 \ll D(H, H)D(H', H')$ . That is, coarse-grained histories corresponding to distinct semiclassical histories tend to decohere.

Note that the degree of decoherence for coarse-grained histories depends on the scale of the coarse graining. Two completely fine-grained histories  $H = C, H' = C'$  do not decohere, as the decoherence functional  $D(H, H')$  is then just equal to the product of their amplitudes  $\mathcal{A}(C)\bar{\mathcal{A}}(C')$ . So some coarse graining is required to get decoherence.

In other words, the computational universe naturally gives rise to a semiclassical spacetime via the decoherent histories approach to quantum mechanics. The computational universe picks out a special set of fine-grained computational histories, corresponding to sequences of projections onto the energy eigenspaces of the quantum logic gates. Each fine-grained computational history gives rise to a spacetime that obeys the Einstein-Regge equations. Coarse graining yields hydrodynamic variables that are coarse-grained averages of the energy-momentum tensor  $T_{ab}$ . Coarse-graining about stable histories yields hydrodynamic variables that approximately decohere and obey classical probabilities.

## 4 Which computation?

Every quantum computation corresponds to a family of metrics, each of which obeys the Einstein-Regge equations. But which computation corresponds to the universe we see around us? What is the ‘mother’ computation? We do not yet know. Candidate computations must be investigated to determine the ones that are compatible with observation.

The ability of quantum computers to simulate lattice gauge theories suggests computations that can reproduce the standard model of elementary particles. Such quantum computations could correspond to quantum cellular automata, with a regular, repeating arrangement of vertices and edges [62-65] (care must be taken to insure that Lorentz in-

variance is preserved [62,66]). The local logic operations in a quantum cellular automaton can be chosen to respect any desired local gauge symmetry such as a Yang-Mills theory. Indeed, the results derived here show how any underlying discrete quantum theory that gives rise to the standard model can be extended to a theory that gives rise not only to the standard model, but to quantum gravity coupled to the standard model as well.

Homogeneity and isotropy for a computational architecture can also be enforced by introducing an element of randomness into the wiring diagram. For example, one can use a random computational graph, as in the theory of causal sets [22-26]; the random arrangement of vertices insures approximate homogeneity and isotropy, in which a coarse-graining containing  $n$  vertices per cell is homogeneous and isotropic to  $O(1/\sqrt{n})$ .

An appealing choice of quantum computation is one which consists of a coherent superposition of all possible quantum computations, as in the case of a quantum Turing machine whose input tape is in a uniform superposition of all possible programs (Methods, section A4). Such a ‘sum over computations’ encompasses both regular and random architectures within its superposition, and weighs computations according to the length of the program to which they correspond: algorithmically simple computations that arise from short programs have higher weight. The observational consequences of this and other candidate computations will be the subject of future work.

## 5 Future work

This paper proposed a theory of quantum gravity derived from quantum computation. I showed that quantum computations naturally give rise to spacetimes that obey the Einstein-Regge equations, with fluctuations in the geometry of the spacetime arising from quantum fluctuations in the causal structure and local action of the computation. This theory makes concrete predictions for a variety of features of quantum gravity, including

the form of the back reaction of metric to quantum fluctuations of matter, the existence of smallest length scales, black hole evaporation, and quantum cosmology. Some of these predictions, such as the absence of spontaneous gravitationally induced decoherence, might be tested soon in the laboratory [42]. In future work, these predictions will be explored in greater detail using numerical simulations to calculate, for example, the spectrum of curvature fluctuations in the early universe.

Because of the flexibility of quantum computation (almost any local quantum system is capable of universal quantum computation), it is a straightforward matter to give models of quantum computation that exhibit a local Yang-Mills gauge invariance. For example, the ‘swap’ picture of quantum computation of section 1.2 above possesses a local  $SU(3) \times SU(2) \times U(1)$  symmetry:  $SU(3) \times U(1)$  commutes with the action of the gates, and  $SU(2)$  commutes with the action of the wires. Whether or not this symmetry can be identified with the  $SU(3) \times SU(2) \times U(1)$  gauge symmetry of the Standard Model is a subject for future work.

*Acknowledgements:* This work was supported by ARDA/ARO, AFOSR, DARPA, NSF, NEC, RIKEN, and the Cambridge-MIT Initiative. The author would like to acknowledge useful conversations with O. Dreyer, F. Dowker, E. Farhi, M. Gell-Mann, V. Giovannetti, J. Goldstone, D. Gottesman, A. Guth, J.J. Halliwell, A. Hosoya, L. Maccone, D. Meyer, F. Marcopoulou, J. Oppenheim, P. Zanardi, and many others.

## References:

- [1] M.A. Nielsen, I.L. Chuang, *Quantum Computation and Quantum Information*, Cambridge University Press, Cambridge, 2000.
- [2] R.P. Feynman, *Int. J. Theor. Phys.* **21**, 467 (1982).
- [3] S. Lloyd, *Science*, **273**, 1073-1078 (1996).
- [4] D.S. Abrams, S. Lloyd, *Phys. Rev. Lett.* **79**, 2586-2589 (1997).
- [5] S. Lloyd, 'Unconventional Quantum Computing Devices,' in *Unconventional Models of Computation*, C. Calude, J. Casti, M.J. Dinneen eds., Springer (1998).
- [6] S. Bravyi., A. Kitaev, *Ann. Phys.* **298**, 210-226 (2002); quant-ph/0003137.
- [7] C. Rovelli, *Quantum Gravity*, Cambridge University Press, Cambridge, 2004.
- [8] S. Carlip, *Rept. Prog. Phys.* **64**, 885 (2001); gr-qc/0108040.
- [9] A. Ashtekar, *Lectures on Non-perturbative Canonical Gravity*, (Notes prepared in collaboration with R.S. Tate), World Scientific, Singapore, 1991.
- [10] G.W. Gibbons, S.W. Hawking, *Euclidean Quantum Gravity*, World Scientific, Singapore, 1993.
- [11] G. 't Hooft, *Class. Quant. Grav.* **16** 3263-3279 (1999), gr-qc/9903084; *Nucl. Phys. B* **342**, 471 (1990).
- [12] J. Wheeler, in *Proceedings of the 3rd International Symposium on Foundations of Quantum Mechanics*, Tokyo (1989); *Geons, Black Holes, & Quantum Foam: A Life in Physics*, by John Archibald Wheeler with Kenneth Ford, W.W. Norton, (1998).

- [13] P.A. Zizzi, *Gen. Rel. Grav.* **33**, 1305-1318 (2001), gr-qc/0008049; gr-qc/0409069.
- [14] J. Polchinski, *String Theory*, Cambridge University Press, Cambridge (1998).
- [15] C. Rovelli, L. Smolin, *Nucl. Phys. B* **331**, 80-152 (1990).
- [16] C. Rovelli, *Phys. Rev. D* **42**, 2638 (1990); *Phys. Rev. D* **43**, 442 (1991); *Class. Quant. Grav.* **8**, 297 (1991); *Class. Quant. Grav.* **8**, 317 (1991).
- [17] C. Rovelli, L. Smolin, *Phys. Rev. D* **52**, 5743-5759 (1995).
- [18] J.C. Baez, *Adv. Math.* **117**, 253-272 (1996).
- [19] J.W. Barrett, L. Crane, *J. Math. Phys.* **39**, 3296-3302 (1998).
- [20] J.C. Baez, J. D. Christensen, T.R. Halford, D.C. Tsang *Class. Quant. Grav.* **19**, 4627-4648 (2002); gr-qc/0202017.
- [21] A.D. Sakharov, *Doklady Akad. Nauk S.S.S.R.* **177**, 70-71 (1967); English translation *Sov. Phys. Doklady* **12**, 1040-1041 (1968).
- [22] L. Bombelli, J. Lee, D. Meyer, R.D. Sorkin, *Phys. Rev. Lett.* **59**, 521-524 (1987).
- [23] X. Matin, D. O'Connor, D. Rideout, R.D. Sorkin, *Phys. Rev. D.* **63**, 084026 (2001).
- [24] G. Brightwell, H.F. Dowker, R.S. Garcia, J. Henson, R.D. Sorkin *Phys. Rev. D* **67**, 08403 (2003); gr-qc/0210061.
- [25] E. Hawkins, F. Markopoulou, H. Sahlmann, *Class. Quant. Grav.* **20** 3839 (2003); hep-th/0302111.
- [26] D. Dou, R.D. Sorkin, *Found. Phys.* **33**, 279-296 (2003); gr-qc/0302009.

- [27] A. Kempf, *Phys. Rev. Lett.* **85**, 2873 (2000), hep-th/9905114; *Phys. Rev. Lett.* **92**, 221301 (2004), gr-qc/0310035.
- [28] D. Finkelstein, *Int. J. Th. Phys.* **27**, 473 (1988).
- [29] A. Marzuoli, M. Rasetti, *Phys. Lett. A* **306**, 79-87 (2002), quant-ph/0209016; quant-ph/0407119; quant-ph/0410105.
- [30] F. Girelli, E.R. Livine, gr-qc/0501075.
- [31] M. Levin, X.-G. Wen, *Rev. Mod. Phys.* **77**, 871-879 (2005), cond-mat/0407140.
- [32] D. Bacon, J. Kempe, D.A. Lidar, K.B. Whaley, *Phys. Rev. Lett.* **85**, 1758-61 (2000), quant-ph/9909058; *Phys. Rev. A* **63**, 042307 (2001), quant-ph/000406.
- [33] D. P. DiVincenzo, D. Bacon, J. Kempe, G. Burkard, K. B. Whaley, *Nature* **408**, 339-342 (2000).
- [34] A. Einstein, *Ann. Physik* **49** (1916), in H.A. Lorentz, A. Einstein, H. Minkowski, H. Weyl, *The Principle of Relativity*, Dover, New York (1952).
- [35] T. Regge, *Nuovo Cimento* **19**, 558-571 (1961).
- [36] W.A. Miller, *Class. Quant. Grav.* **14** L199-L204 (1997); gr-qc/9708011.
- [37] R. Friedberg, T.D. Lee, *Nucl. Phys. B* **242**, 145-166 (1984).
- [38] A. Okabe, B. Boots, K. Sugihara, *Spatial Tessellations: Concepts and Applications of Voronoi Diagrams*, Wiley, Chichester (1992).
- [39] S.W. Hawking, G.F.R. Ellis, *The Large Scale Structure of Space-Time*, Cambridge University Press, Cambridge, 1973.

- [40] J.B. Hartle, R. Sorkin, *Gen. Rel. Grav.* **13**, 541-549 (1981).
- [41] J. Ambjorn, J. Jurkiewicz, R. Loll, *Phys. Rev. Lett.* **93**, 131301 (2004); hep-th/0404156.
- [42] W. Marshall, C. Simon, R. Penrose, D. Bouwmeester, *Phys. Rev. Lett.* **91**, 130401 (2003); quant-ph/0210001.
- [43] S. Lloyd, “Almost certain escape from black holes,” quant-ph/0406205. To appear in *Phys. Rev. Lett.*
- [44] G.T. Horowitz and J. Maldacena, “The Black-Hole Final State,” hep-th/0310281.
- [45] D. Gottesman and J. Preskill, “Comment on ‘The black hole final state,’ ” hep-th/0311269.
- [46] U. Yurtsever and G. Hockney, “Causality, entanglement, and quantum evolution beyond Cauchy horizons,” quant-ph/0312160.
- [47] U. Yurtsever and G. Hockney, “Signaling and the Black Hole Final State,” quant-ph/0402060.
- [48] V. Giovannetti, S. Lloyd, L. Maccone, *Science* **306**, 1330 (2004), quant-ph/0412078; quant-ph/0505064.
- [49] J.D. Bekenstein, *Phys. Rev. D* **7**, 2333 (1973); *Phys. Rev. D.* **23**, 287 (1981); *Phys. Rev. Letters* **46**, 623 (1981); *Phys. Rev. D.* **30**, 1669-1679 (1984).
- [50] G. 't Hooft, “Dimensional reduction in quantum gravity,” gr-qc/9310026.
- [51] L. Susskind, *J. Math. Phys.* **36**, 6377, hep-th/9409089.

- [52] Linde, A., *Particle Physics and Inflationary Cosmology*, Harwood Academic, New York (1990).
- [53] R. Griffiths, *J. Stat. Phys.* **36**, 219 (1984).
- [54] R. Omnés, *J. Stat. Phys.* **53**, 893, 933, 957 (1988); *J. Stat. Phys.* **57**, 359 (1989); *Rev. Mod. Phys.* **64**, 339 (1992); *The Interpretation of Quantum Mechanics*, Princeton University Press, Princeton, 1994.
- [55] M. Gell-Mann, J.B. Hartle *Phys. Rev. D* **47**, 3345-3382 (1993); gr-qc/9210010.
- [56] J.J. Halliwell, *Phys. Rev. D* **58** 105015 (1998), quant-ph/9805062; *Phys. Rev. D* **60** 105031 (1999), quant-ph/9902008; *Phys. Rev. Lett.* **83** 2481 (1999), quant-ph/9905094; ‘Decoherent Histories for Spacetime Domains,’ in *Time in Quantum Mechanics*, edited by J.G.Muga, R. Sala Mayato and I.L.Egusquiza (Springer, Berlin, 2001), quant-ph/0101099.
- [57] J.J. Halliwell, J.Thorwart, *Phys. Rev. D* **65** 104009 (2002); gr-qc/0201070.
- [58] J.B. Hartle, *Phys. Scripta* **T76**, 67 (1998), gr-qc/9712001.
- [59] F. Dowker and A. Kent, *Phys. Rev. Lett.* **75**, 3038 (1995).
- [60] A. Kent, *Physica Scripta* **T76**, 78 (1998).
- [61] T.A. Brun, J.B. Hartle, *Phys. Rev. E***59**, 6370-6380 (1999), quant-ph/9808024; *Phys. Rev. D***60**, 123503 (1999), quant-ph/9905079.
- [62] I. Bialynicki-Birula, *Phys. Rev. D* **49**, 6920-6927 (1994); hep-th/9304070.

[63] Margolus, N., *Ann. N.Y. Acad. Sci.* **480**, 487-497 (1986); and in *Complexity, Entropy, and the Physics of Information*, vol. VIII, W. H. Zurek, ed., pp. 273-87, Addison-Wesley, Englewood Cliffs 1990.

[64] R.P. Feynman, *Rev. Mod. Phys.* **20**, 267 (1948); R.P. Feynman, A.R. Hibbs, *Quantum Mechanics and Path Integrals*, McGraw-Hill, New York, 1965.

[65] B. Gaveau, T. Jacobson, M. Kac, L.S. Schulman, *Phys. Rev. Lett.* **53**, 419 (1984).

[66] F. Dowker, J. Henson, R.D. Sorkin, *Mod. Phys. Lett. A* **19** 1829-1840 (2004); gr-qc/0311055.

## 6 Supporting online material: Methods

### 6.1 Introduction

Note that while the computational universe program is not obviously related to string theory and loop quantum gravity, it is not necessarily incompatible with these approaches. (For work relating quantum computation to loop quantum gravity see [13, 29-30].) First of all, to the extent that the dynamics of these theories are discrete and local, they can be efficiently reproduced on a quantum computer. So, for example, a quantum computer can reproduce the dynamics of discretized conformal field theories, which should allow the simulation of string theory in the anti-de Sitter/conformal field theory (AdS/CFT) correspondence. In addition, it is likely that string theory and loop quantum gravity are themselves computationally universal in the sense that they can enact any quantum computation. (Computational universality is ubiquitous: most non-trivial dynamics are computationally universal.) If this is so, it is possible that all of these approaches to quantum gravity are logically equivalent in the same sense that a Macintosh is logically equivalent to a PC which in turn is logically equivalent to a Turing machine.

Such logical equivalence need not necessarily imply *physical* equivalence, however. Computation has consequences: it induces spacetime curvature. In the model of quantum gravity presented here, the extra computation required to reproduce string theory from an underlying computation or from loop quantum gravity might in principle be detectable. This issue will be discussed further below.

The idea of deriving gravity from an underlying quantum theory is reminiscent of Sakharov's work deriving gravity from an underlying elastic medium [21]. Unlike [21], however, the theory presented here presents an explicit mechanism for the back reaction of gravity to quantum fluctuations in the underlying matter.

## 6.2 The computational graph

As just noted, there are many different models of universal quantum computation, all logically equivalent to each other in the sense that each model can simulate the others efficiently (it is even possible to have quantum circuit models that admit closed cycles) [1]. The quantum circuit model for quantum computation adopted here is the model most closely related to the structure of events in spacetime.

Many models of quantum computation use single-qubit operations. For example, a popular model uses single-qubit rotations together with controlled-NOT operations or swap operations [1]. Single-qubit rotations together with swap operations possess an  $SU(2)$  gauge symmetry which makes this model richer and more complex than the basic two-qubit logic gate model discussed here. Quantum computation with gauge symmetries is related to computational models of elementary particles and will be discussed elsewhere. The addition of single-qubit logic gates will be discussed in section A2.3 below.

Note that for a quantum computer to be able to simulate fermionic systems efficiently, it should have access to fermionic degrees of freedom [2-6]. This is consistent with the

identification of qubits with spin-1/2 massless particles. Fermionic statistics can be enforced either by defining quantum logic gates in terms of anti-commuting creation and annihilation operators [5], or by using appropriate local interactions [6,31] which enforce fermionic statistics dynamically.

### 6.3 Computational histories

In the example given in section (1.2), for simplicity we took the lowest eigenvalue to be zero and the only non-zero eigenvalue to be 1. For the generic case in which quantum logic gates have Hamiltonians with more than one non-zero eigenvalue, there is more than one kind of scattering event. Because only the relative phase is observable, we take the lowest eigenvalue to be zero and the other eigenvalues to be positive. The zero eigenvalue still corresponds to non-scattering non-events; but now when scattering occurs, the qubits can acquire different phases, one for each non-zero eigenvalue. The number of causal structures is the same as discussed in section (1.2) (i.e.,  $2^n$ , where  $n$  is the number of gates), but now each causal structure gives rise to a number of different computational histories at each gate, each with a different action corresponding to the different phase for each non-zero eigenvalue. If there are  $m$  distinct eigenvalues per gate, then there are  $m^n$  computational histories.

Taking the eigenvalues of the Hamiltonian and phases to be non-negative insures the positivity of the energy of interaction in quantum logic gates as measured locally. More precisely, as shown in section (A2.2) below, it assures the negativity of  $T^a_a$  and the positivity of curvature. That is, the local non-negativity of the energy of interaction within a quantum logic gate insures a version of the strong energy condition ([39] section 4.3).

If acquired phases and local energies can be negative, then the procedure of assigning

a metric to spacetime based on the underlying quantum computation still holds. Now, however, it is possible to fit arbitrarily large amounts of computation into a volume of spacetime without generating any curvature on average, merely by having the average angle rotated within the volume be zero. The inclusion of negative local energies and phases has implications for holography and quantum cosmology and will be discussed further in section 3 below.

The relationship between the overall computational graph and that of the individual computational histories works as follows. Each logic gate has two inputs,  $A$  and  $B$ , and two outputs,  $A'$  and  $B'$ . The inputs  $A$  and  $B$  come from outputs  $A_{\text{out}}$  and  $B_{\text{out}}$  of other gates, and the outputs  $A'$  and  $B'$  are inputs to  $A_{\text{in}}$  and  $B_{\text{in}}$  of other gates. In the case that there is scattering, there is a vertex at the gate. In the case of no scattering, delete the vertex and connect  $A_{\text{out}}$  directly to  $A_{\text{in}}$ , and  $B_{\text{out}}$  directly to  $B_{\text{in}}$ . The new connections are null lines in the computational history where there is no scattering at that gate.

The process of excising a gate to construct a new computational history can be thought of as follows: the gate is cut out, the cut lines are re-connected to the appropriate ends, and then they ‘spring tight’ to give null lines in the new computational history from which the non-scattering vertex has been deleted.

## 6.4 Constructing a Simplicial Lattice

A computational history does not form a simplicial lattice in itself, but it can be extended to a simplicial lattice by adding additional edges, and, if necessary, vertices. There are a variety of ways to extend a graph to a simplicial lattice [38]. Here we discuss two, but more are possible. Both constructions are based on dual Delaunay and Voronoi lattices. Method 1 results in a discretized manifold that is topologically equivalent to  $R^4$ , but requires the addition not only of more edges, but of more vertices as well. Method 2 does

not require additional vertices to be added, but typically results in a topologically non-trivial discretized manifold. The important feature of the different possible triangulations is that all possible ways of extending the computational history into a simplicial lattice,  $D_C$ , result in spacetimes that are equivalent in terms of their observable content, i.e., their causal structure, action, and curvature. Accordingly, one may adopt whichever triangulation is convenient for a particular problem.

*Method 1*

(1) Embed the computational history in  $R^4$  via an embedding mapping  $\chi(C)$  that maps vertices to points in  $R^4$  and wires to line segments in the manifold connecting the vertices, as above.

(2) Construct the Voronoi lattice  $V_C$  for the vertices of  $\chi(C)$  by dividing spacetime into regions that are closer to one vertex of  $C$  than to any other vertex. Here, ‘closer’ is defined using the ordinary Euclidean metric on the manifold. The Voronoi lattice defines the volumes associated with vertices of the computational graph.

(3) Connect vertices of the computational graph to neighboring vertices through the centroids of faces of the Voronoi lattice to form the Delaunay lattice  $D_C$  dual to  $V_C$ .  $D_C$  is the simplicial lattice that will be used to define the Regge calculus. (In some degenerate cases of measure 0,  $D_C$  is not simplicial; in these cases a slight change in the embedding will render  $D_C$  simplicial.) The faces of the Voronoi lattice bisect the edges of the Delaunay lattice.

(4) Check to make sure that the original edges of the computational history are edges of  $D_C$ . If they are not, simply add new, ‘reference’ vertices along the edges of  $C$  and repeat steps 1 – 3. By making the reference vertices sufficiently close together, this procedure insures that all edges of  $C$  fall along edges of  $D_C$ . In particular, if the reference vertices

along a given are closer to their neighbors along the edge than to any other vertices, then every edge of  $C$  is guaranteed to lie along edges of  $D_C$ . The reference vertices will in general divide the original edges of  $C$  into several segments.

Steps (1-4) are a standard procedure for constructing a simplicial Delaunay lattice together with its dual Voronoi lattice.

Some authors exhibit a prejudice against the use of highly elongated simplices in a Delaunay lattice [38]. If desired, further reference vertices can be added in ‘empty space’ to construct a Delaunay lattice without elongated simplices. Once again, just as different surveyors can choose different triangulations for the same landscape, the precise arrangement of added edges and vertices does not affect the observable content of the spacetime. These additional edges and vertices are ‘fictions’ that we use to fill in a simplicial geometry: the lengths of these added edges are derived from the underlying observational content. In contrast, the ‘factual’ content of the geometry lies in its causal structure and local actions.

Note that if we choose to add additional reference vertices, we must give a method for assigning the as yet unknown terms of the metric at those vertices. That method is closely analogous to the technique for assigning the unknown terms of the metric at the vertices of the computational history and will be given in section A2.3 below.

### *Method 2*

Method 1 for constructing a simplicial lattice results in a discretized manifold that is topologically equivalent to  $R^4$  or to a convex subset of  $R^4$ . A second way of extending the computational history to a simplicial lattice requires no additional reference vertices, but can result in a discretized manifold that is not simply connected. Once again, the resulting lattice gives a spacetime with the same causal structure, action, and curvature as method 1, i.e., any difference in the topology of the different lattices is observationally

undetectable.

In method 2, to construct a simplicial lattice corresponding to the discrete computational history, consider not just one embedding map  $\chi$ , but a sequence of embedding maps  $\{\chi_\ell\}$ . Each embedding map  $\{\chi_\ell\}$  embeds a vertex  $\ell$  in  $R^4$  together with a neighborhood  $\nu_\ell$  of nearby vertices, including its neighbors and next-to-nearest neighbors.  $\chi_\ell$  is one chart in the atlas of embedding maps  $\{\chi_\ell\}$  that defines the discretized manifold. Now, once again, use the Delaunay/Voronoi construction to produce a simplicial lattice for the vertices in the neighborhood. Because there are only a small number of vertices in the neighborhood, it is always possible to choose the embedding so that each edge in the neighborhood is an edge in the Delaunay lattice. Similarly, in the embeddings can always be chosen to give the same set of Delaunay edges and Voronoi volumes in the overlap  $\nu_\ell \cap \nu_{\ell'}$  between two adjacent vertices  $\ell$  and  $\ell'$ . The resulting atlas of overlapping charts, together with the accompanying Delaunay and Voronoi lattices, defines the discretized manifold  $M_C$ . Note that in this construction no new reference vertices are required.

The price of adding no reference vertices is that the resulting discretized manifold may no longer be simply connected. In method 2, simple, locally-connected computations such as quantum cellular automata typically give rise to low genus  $M_C$ , while more complex computations with long-distance connections can give rise to manifolds with high genus.

No matter how the computational history is extended to a simplicial lattice, the resulting discrete spacetime possesses the same causal structure and action. As will now be seen, it also possesses the same curvature at each vertex.

## 6.5 Regge Calculus

The four null lines at each vertex of the computational graph set four out of the ten components of the metric in four dimensions (i.e., in the null basis given by the lines, the

on-diagonal parts of the metric are zero). The four null lines at each vertex define six planes, one for each pair of lines and for each of the undetermined off-diagonal components of the metric. Two of these planes – the plane defined by the two ingoing null lines, and the one defined by the two outgoing null lines – contain vectors that are timelike with respect to the vertex. The remaining four – defined by one ingoing and one outgoing line – contain spacelike vectors. Each plane corresponds to an off-diagonal term in the metric.

Because quantum logic gates have two inputs and two outputs, four dimensions arise naturally in the computational universe. The local null tetrad over-determines the metric in fewer than four dimensions, and under-determines it in more than four dimensions. In the computational universe, the four-dimensional structure of spacetime arises out of pairwise interactions between information-bearing degrees of freedom. Note that as in [41] one must still verify that a microscopically four-dimensional spacetime still looks four-dimensional at macroscopic scales.

## 6.6 The Einstein-Regge equations

To obtain the explicit form of the Einstein-Regge equations,  $\delta I_G/\delta g_{ab}(\ell) + \delta I_C/\delta g_{ab}(\ell) = 0$ , recall that the gravitational action is  $I_G = (1/8\pi G) \sum_h \epsilon_h A_h$ , where  $\epsilon_h$  is the deficit angle of the hinge  $h$  and  $A_h$  is its area. Under a variation of the metric at point  $\ell$ ,  $g_{ab}(\ell) \rightarrow g_{ab}(\ell) + \delta g_{ab}(\ell)$ , the variation in the gravitational action is given by Regge [12]:

$$\delta I_G = \frac{1}{8\pi G} \sum_h \epsilon_h \delta A_h \tag{16}$$

$$= \frac{1}{16\pi G} \sum_h \sum_{p(h)} l_{ph} \delta l_{ph} \cotan \phi_{ph}. \tag{17}$$

Here, as Regge showed, the variation in  $\epsilon_h$  cancels out,  $l_{ph}$  is the  $p$ 'th edge of hinge  $h$  ( $p=1,2,3$ ), and  $\phi_{ph}$  is the angle in the hinge opposite to  $l_{ph}$ .

Explicitly inserting the variation in the metric, we obtain

$$\delta I_G = \frac{1}{8\pi G} \sum_h \epsilon_h \frac{\delta A_h}{\delta g_{ab}} \delta g_{ab} \quad (18)$$

$$= \frac{1}{16\pi G} \sum_h \sum_{p(h)} l_{ph} \frac{\delta l_{ph}}{\delta g_{ab}} \delta g_{ab} \cotan \phi_{ph}. \quad (19)$$

Combining equation this equation with equation (2.2) for the variation of the action of the computational matter with respect to the metric gives

$$- \sum_{h \in N(\ell)} \sum_{p(h)} l_{ph} \frac{\delta l_{ph}}{\delta g_{ab}(\ell)} \cotan \phi_{ph} = 8\pi G (\hat{T}^{ab} - \mathcal{U}_\ell g^{ab}(\ell)) \Delta V_\ell. \quad (20)$$

Here, the sum over hinges includes only hinges  $h \in N(\ell)$  that adjoin the vertex  $\ell$ , as the edges of other hinges do not change under the variation of the metric at  $\ell$ . More succinctly, we have

$$- \sum_{h \in N(\ell)} \epsilon_h \frac{\delta A_h}{\delta g_{ab}} = 4\pi G T^{ab} \Delta V_\ell \quad (21)$$

This is the expression of the Einstein-Regge equations in the computational universe.

## 6.7 Satisfying the Einstein-Regge equations

In sections 2.2-2.3, all vertices in the simplicial lattice were assumed to be vertices of the computational history, as in method 2 above. That is, each vertex has four null edges, corresponding to two incoming and two outgoing quantum degrees of freedom. For method 1, we have to assign the unknown components of the metric and of the energy-momentum tensor at reference vertices where there is only one null line, corresponding to a single edge of the computational history, or no null lines, corresponding to a reference vertex put down in ‘empty space.’

For the case of a reference vertex with one null line  $E_1$ , simply proceed as in section 2.2. Using that null line as one vector in a basis at that vertex, we see that only one

on-diagonal term in the metric is known, e.g.,  $g_{11} = 0$ . The remaining on-diagonal terms and the off-diagonal terms are to be assigned by the requirement of self consistency, as before. At a reference vertex, the action of the ‘computational matter’ is zero, and the only non-zero term in the energy momentum tensor is the 11 kinetic energy term:  $\hat{T}^{ab} = \gamma_1 E_1^a E_1^b$ . This term corresponds to a single massless particle propagating in the  $E_1$  direction. Here also, the value of the particle’s kinetic energy density,  $\gamma_1$ , is to be determined by self-consistency. To satisfy the Einstein-Regge equations (2.3), first assign the unknown terms of the metric at the vertex to make all but the 11 term in equation (2.3) hold. The metric is now completely determined. Next, assign the kinetic energy density  $\gamma_1$  to make the 11 component of (2.3) hold. The Einstein-Regge equations are now satisfied at the reference vertex.

Initial and final states of the computation correspond to vertices that have only one null line emerging from them (initial states) or leading to them (final states). If the initial and final states are two-particle singlet states, then they have two null lines emerging from them or leading to them. The method for satisfying the Einstein-Regge equations at such points is essentially the same as for the reference vertices of the previous paragraph. The null line or lines at the vertex determines part of the metric at that point; select the remaining parts of the metric to insure that the Einstein-Regge equations hold for the remaining parts of the metric at that point. (Here one must be sure to include the boundary terms [40] in the action.) Then assign the kinetic energies for the null lines to make the rest of the Einstein-Regge equations hold.

The case of a reference vertex in ‘empty space’ is even simpler. Here, nothing is known about the metric *a priori*. All the terms in the energy-momentum tensor are zero. Equation (2.3) is then a ten-component equation in the ten unknown components of the metric. Solving equation (2.3) assigns those components in a self-consistent fashion.

Essentially, in parts of spacetime where there are no logic gates or quantum wires, i.e., no information and no information processing, we assign the metric by solving the vacuum Regge equations. In the absence of computational ‘matter,’ the only part of the curvature tensor that is non-zero is the Weyl tensor, corresponding to gravity waves. As usual in general relativity, the sources of those gravity waves are places where there is matter, and the Ricci tensor and curvature scalar are non-zero (see [39], section 4.1, and section 3 below). Note that gravity waves are not quantized directly in this theory: instead, their presence is deduced by their interactions with the computational matter.

## 6.8 Single qubit quantum logic gates

Single qubit quantum logic gates with one input and one output can be accommodated in the theory in a method similar to that used in the preceding paragraphs. A single-qubit gate gives rise to several different computational histories, one corresponding to each distinct eigenvalue of the gate’s unitary operator. For the zero eigenvalue (no action), there is no vertex in the computational history associated with the gate, and the input and output edges of the gate are joined into a single edge, corresponding to a single null line in the computational spacetime. For non-zero eigenvalues  $\theta$ , the gate gives rise to a vertex with action  $-\hbar\theta$  in the computational history. The input and output lines then correspond to two linearly independent null lines in the spacetime.

These two lines define two of the components of the metric: the on-diagonal terms corresponding to the two lines are zero. Choose the remaining eight components of the metric to make the corresponding eight components of the Einstein-Regge equations (2.3) hold. Finally, choose the kinetic energy terms for the ‘particles’ travelling along those two null lines to make the remaining two components of the Einstein-Regge equations hold.

## 6.9 Comparison with GPS

The procedure described in section 2.3 for inferring the off-diagonal part of the metric and the traceless part of the energy-momentum tensor is analogous to classical procedures for determining the geometry of spacetime from the behavior of matter within that spacetime [39]. The reconstruction of the metric from the null lines and the local action at each vertex closely resembles the way that a swarm of GPS satellites maps out spacetime geometry by sending signals along null lines and timing their arrival by counting the ticks of their local clocks [48]. In the method for reconstructing the metric detailed here, a ‘tick’ of a clock corresponds to a local accumulation of an angle  $\pi$  at a quantum logic gate.

The method for reconstructing spacetime geometry given here is slightly more complicated than the reconstruction of geometry from GPS data, however, because we also have to determine the form of the energy-momentum tensor. In particular, the atomic clocks in GPS satellites rely on the fact that all the atoms in the clock have well-characterized hyperfine energy level splittings that are in principle identical from atom to atom. Here, we don’t know the energy and time scales corresponding to a given quantum logic gate until the length scale, as embodied by the conformal factor, has been assigned at each gate. Still, as shown above, exactly enough information is embodied in the behavior of the computational ‘matter’ – where it goes, and what it does when it gets there – to deduce the full metric and the energy-momentum tensor.

## 6.10 Coarse graining and the Einstein equations

Every computational history corresponds to a spacetime that obeys the Einstein-Regge equations. The overall quantum computation is the sum of individual computational histories corresponding to different causal structures. Fluctuations in space and time

track the quantum fluctuations in the local routing of information and action accumulated at each quantum logic gate.

Solving (2.3) to assign the off-diagonal part of the metric and the on-diagonal part of the energy-momentum tensor involves solving a nonlinear partial difference equation, and then determining the on-diagonal part of the energy-momentum tensor from the remainder of the Einstein-Regge equations. Future work will involve solving (2.3) directly in order to investigate the behavior of the computational universe at the smallest scales.

The underlying dynamics in the computational universe is given by Regge calculus. Einstein's equations are known to follow from Regge calculus by a procedure of coarse graining [35]. This coarse-grained picture proceeds as follows. Coarse grain spacetime by averaging over a cell size  $\zeta$  where the volume  $dv \equiv \zeta^4$  in the coarse graining contains many points in the computational graph. Then construct a coarse-grained metric  $g_{ab}(x)$ , and coarse-grained curvatures  $R(x)$  and Lagrangians  $\mathcal{L}(x)$  by averaging over those coarse-grained volumes.

As Regge noted (and as is true for all coarse grainings of discrete equations) care must be taken to insure that the coarse-grained equations accurately reflect the true behavior of the underlying discrete dynamics. Such a coarse grained picture should be reasonably accurate when (1) The underlying computational graph is relatively homogeneous, as it is for cellular automata and homogeneous random architectures. (2) The curvature is significantly smaller than the inverse Planck length squared. (3) The variation of the average angle rotated per coarse-grained cell is small from cell to cell.

Note that the quantum computations that reproduce homogeneous, local quantum theories such as lattice gauge theories obey all three of these requirements.

Coarse graining is a useful tool for analyzing nonlinear discrete systems such as those considered here. But the realm of validity of coarse graining for nonlinear systems is a

subtle subject; although heuristic arguments like those above can give some confidence in the application of coarse graining, in the final analysis its validity must be tested by comparing coarse-grained solutions with the complete solution of the underlying discrete dynamics. In the computational universe, to analyze scenarios such as initial and final singularities where quantum gravity truly comes into play, the underlying equations must be solved directly.

With these caveats in mind, now follow the procedure for deriving the Einstein-Regge calculus above, but in the coarse-grained context. In the coarse-grained setting, our equations take the conventional Einstein form:

$$R_{ab} - \frac{1}{2}g_{ab}R = 8\pi G(\hat{T}_{ab} - g_{ab}\mathcal{U}) = 8\pi GT_{ab}. \quad (22)$$

We proceed as for the discrete case. The underlying computational graph gives us four null lines at each point, fixing the on-diagonal parts of the metric to zero in a coordinate system for which those lines form a basis. Assign the six unknown off-diagonal parts of the metric to make the off-diagonal part of the Einstein equations hold. The left-hand side of the Einstein equations is now completely determined. Once the off-diagonal part of the metric has been obtained, the on-diagonal kinetic energy terms  $\hat{T}^{ab}$  can be obtained as before by assigning them so that the on-diagonal part of Einstein's equations are obeyed. The full Einstein equations now hold.

To assign the metric uniquely so that make Einstein's equations hold globally, boundary conditions must be supplied for equation (A2.4). At the initial and final points of the computation, the metric is incompletely defined, corresponding to a singularity in the equations. This suggests setting boundary conditions by taking  $\Omega = 0$  at these points. In the case of an infinite computation, with no final points, one can set boundary conditions by taking  $\Omega = 0$ ,  $\Omega_{;a} = 0$  at initial points.

## 6.11 Which computation?

This paper showed that any computation, including, for example, one that calculates the digits of  $\pi$ , corresponds to a class of spacetimes that obeys the Einstein-Regge equations. Which computation corresponds to the world that we see around us? As noted, quantum cellular automata and random computations are both reasonable candidates for the ‘universal’ computation. Cellular automata possess a built-in regular structure which simplifies the analysis of their behavior. A quantum cellular automaton is a natural choice for a computational substrate, although care must be taken in the choice of the arrangement of cells to insure that light propagates at a uniform rate in all directions. Bialynicki-Birula has shown that the Weyl, Dirac, and Maxwell equations can be recovered from quantum cellular automata on body-centered cubic lattices [62].

A hyper-diamond lattice consisting of 4-cubes stacked with their longest diagonal along the ‘time’ direction also represents a natural lattice in which to embed a CA-like architecture. (I am indebted to R. Sorkin for calling this lattice to my attention.) Each vertex has four inputs and four outputs. Label inputs and outputs from 1 to 4. The lattice can be filled alternately with gates that have their two inputs on even lines and their two outputs on odd lines, and gates that have their two inputs on odd lines and their two outputs on even lines. Lattice gauge theories can be described readily either by the body-centered cubic lattices of [62] or by hyper-diamond lattices.

Similarly, a fully random computational graph with  $n$  vertices can be analyzed using statistical techniques. Such a graph possesses a locally tree-like structure; the smallest loops are of size order  $\log n$ ; and the average loop has size  $\sqrt{n}$ . Because the smallest loop size gets larger and larger as  $n \rightarrow \infty$ , a random computational graph gives a geometry that is locally approximately flat. Random graphs tend to have a complex topology, while CA-like architectures have a simple topology.

It must be admitted, however, that in investigating quantum cellular automata and random graphs, we do so exactly because they have symmetries or statistical regularities that simplify the analysis. In point of fact, we do not know what form of the ‘mother computation’ takes. Rather, we should investigate different candidates and compare the results of those investigations with observation.

In fact, computational universality — the ability of quantum computers to simulate each other efficiently — suggests that it may not be so important which computation we use. Computational universality allows a quantum computer to give rise to all possible computable structures. Consider, for example, a quantum Turing machine whose input tape is prepared in an equal superposition of all possible programs. (In fact, almost any input state for the tape will give rise to an almost equal superposition of all possible programs). The amplitude for a given input program of length  $\ell$  is then just equal to  $2^{-\ell/2}$ . Such a quantum computer will produce all possible outputs in quantum superposition, with an amplitude for each output equal to the sum of the amplitudes for the programs that produce that output:  $\mathcal{A}(o) = \sum_{p:U(p)=o} 2^{-\ell_p/2} \mathcal{A}_p$ .  $\mathcal{A}(o)$  is the *algorithmic amplitude* for the output  $o$ . Here,  $\mathcal{A}_p$  is defined as in section (1) to be the amplitude that the computation starting from program  $p$  actually gives the output  $o$ .

To relate the quantum Turing machine picture to the quantum circuit picture described here, consider a quantum Turing machine whose outputs are quantum circuits. The circuits generated by such a machine constitutes a ‘family.’ Some of the circuits in the family could be infinite, even if the program producing them is finite in length. A uniform superposition of inputs for such a Turing machine produces a superposition of quantum circuits, each weighted by their algorithmic amplitude.

Because of computational universality, algorithmic amplitude is approximately machine independent: each universal quantum computer can be programmed simulate any

other quantum computer by a program of finite length. As a result, the algorithmic amplitude of an output on one universal quantum computer differs by at most a constant multiplicative factor from the algorithmic amplitude of the output on another universal quantum computer (compare the analogous classical result for algorithmic probability). Regular circuits such as CAs that produce simple dynamical laws have high weight in the universal family because they are produced by short programs.

Such a universal quantum computer that computes all possible results, weighted by their algorithmic amplitude, preferentially produces simple dynamical laws. Our own universe apparently obeys simple dynamical laws, and could plausibly be produced by such a universal quantum computer.

Quantum computational universality is a powerful feature: it is what allows the computational universe to reproduce the behavior of any discrete, local quantum system, including lattice gauge theories. But care must be taken in applying this power. In particular, to reproduce a lattice gauge theory, a quantum computation uses quantum logic gates to reproduce the local infinitesimal Hamiltonian dynamics. If those logic gates possess the same gauge symmetries as the theory to be simulated, then the action of the logic gates can be the same as the action of the simulated theory, and the dynamics of the simulation can be essentially indistinguishable from the dynamics of the system simulated. This is the situation envisaged by Feynman in his paper on universal quantum simulation [2]. For example, as noted above, the simple ‘swap’ model of quantum computation presented in section (1) possesses a local  $SU(3) \times U(1)$  symmetry at each logic gate, corresponding to transformations on the triplet and singlet subspaces, together with a local  $SU(2)$  symmetry on the wires. Whether this local  $SU(3) \times SU(2) \times U(1)$  symmetry can be identified with the  $SU(3) \times SU(2) \times U(1)$  Yang-Mills gauge symmetry of the standard model will be investigated elsewhere.

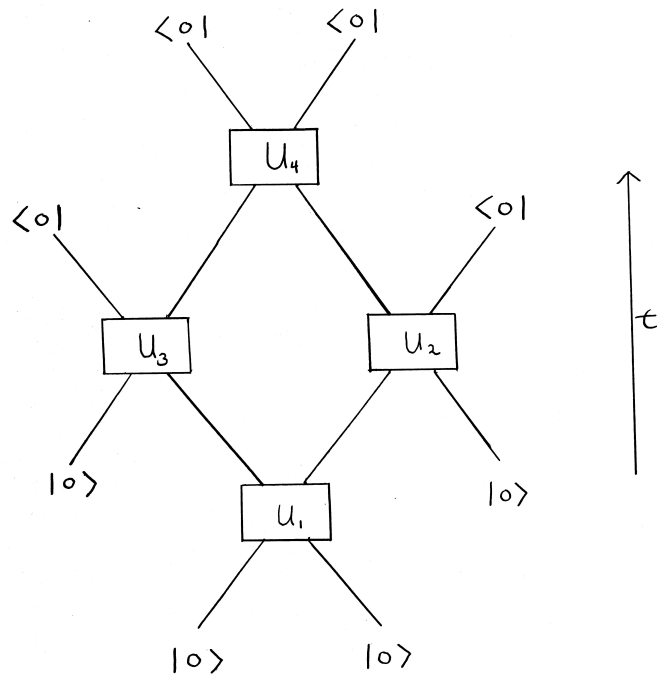


Figure 1

Figure 1: A quantum computation corresponds to a directed, acyclic graph. Initial vertices correspond to initial states  $|0\rangle$ ; edges correspond to quantum wires; internal vertices correspond to quantum logic gates that apply unitary transformations  $U_\ell$ ; final vertices correspond to final states  $\langle 0|$ .

$$\begin{array}{c}
 \begin{array}{c} \diagup \\ \boxed{u} \\ \diagdown \end{array} = \begin{array}{c} \diagup \\ \times \\ \diagdown \end{array} + \begin{array}{c} \diagup \\ \circ \\ \diagdown \end{array} \\
 U = e^{-i\theta P} = 1 - P + P e^{-i\theta}
 \end{array}$$

Figure 2

Figure 2: As qubits pass through a quantum logic gate, they can either scatter or not. If they scatter, then their state acquires a phase  $\theta$ ; if they don't scatter, no phase is acquired. Scattering corresponds to an 'event'; no scattering corresponds to a 'non-event.'

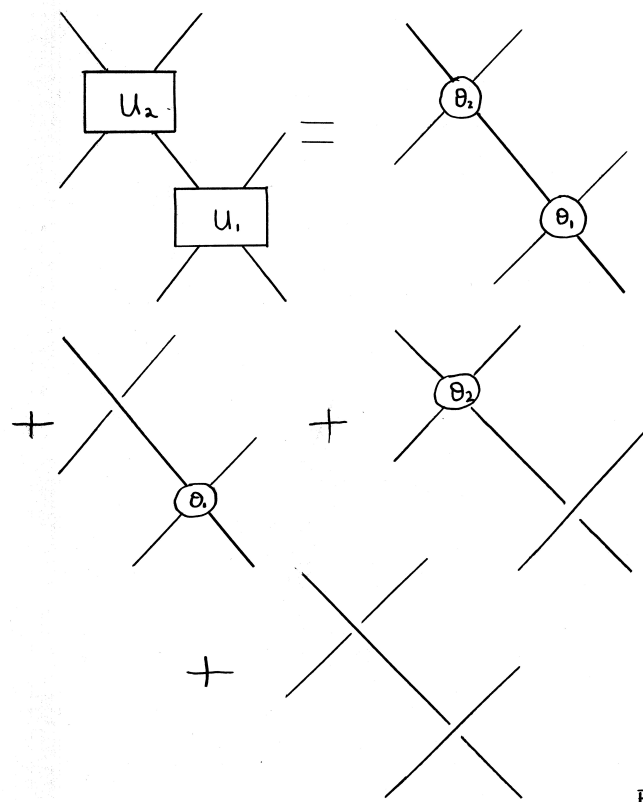


Figure 3

Figure 3: A quantum computation can be decomposed into a superposition of computational histories, each of which corresponds to a particular pattern of scattering events. Each computational history in turn corresponds to a spacetime with a definite metric.

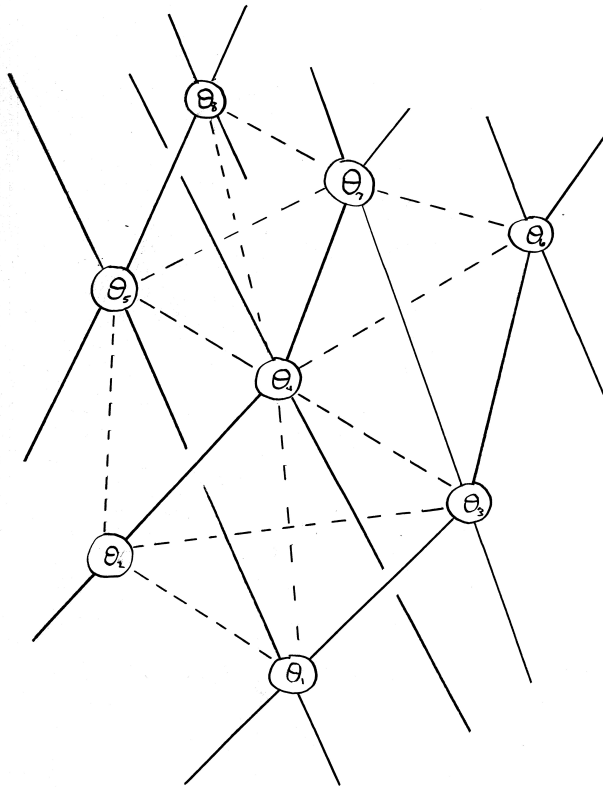


Figure 4

Figure 4: To construct a discretized spacetime from a computational history, add edges and vertices to form a simplicial ‘geodesic dome’ lattice. Figure 4a shows the four-simplex associated with a vertex and its nearest neighbors. Figure 4b shows a triangulation of a computational history, analogous to the triangulation performed by a surveyor who adds additional reference vertices and edges to construct a simplicial lattice. Edge lengths are defined by the causal structure of the computational history, together with the local action  $\hbar\theta_\ell$  of the underlying computation. The resulting discrete geometry obeys the Einstein-Regge equations.